ORNL/SPR-2023/2918

FY23 ARPA-E Milestone Report
ULTIMATE FY22 Creep Test Facility Report

Approved for public release.
Distribution is unlimited.

B. A. Pint
S. Dryepondt

May 2023

OAK RIDGE NATIONAL LABORATORY
MANAGED BY UT-BATTELLE FOR THE US DEPARTMENT OF ENERGY

DOCUMENT AVAILABILITY

Reports produced after January 1, 1996, are generally available free via US Department of Energy (DOE) SciTech Connect.

Website http://www.osti.gov/scitech/

Reports produced before January 1, 1996, may be purchased by members of the public from the following source:

National Technical Information Service
5285 Port Royal Road
Springfield, VA 22161
Telephone 703-605-6000 (1-800-553-6847)
TDD 703-487-4639
Fax 703-605-6900
E-mail info@ntis.gov
Website http://www.ntis.gov/help/ordermethods.aspx

Reports are available to DOE employees, DOE contractors, Energy Technology Data Exchange representatives, and International Nuclear Information System representatives from the following source:

Office of Scientific and Technical Information
PO Box 62
Oak Ridge, TN 37831
Telephone 865-576-8401
Fax 865-576-5728
E-mail reports@osti.gov
Website http://www.osti.gov/contact.html

This report was prepared as an account of work sponsored by an agency of the United States Government. Neither the United States Government nor any agency thereof, nor any of their employees, makes any warranty, express or implied, or assumes any legal liability or responsibility for the accuracy, completeness, or usefulness of any information, apparatus, product, or process disclosed, or represents that its use would not infringe privately owned rights. Reference herein to any specific commercial product, process, or service by trade name, trademark, manufacturer, or otherwise, does not necessarily constitute or imply its endorsement, recommendation, or favoring by the United States Government or any agency thereof. The views and opinions of authors expressed herein do not necessarily state or reflect those of the United States Government or any agency thereof.

ULTIMATE FY22 Creep Test Facility Report

B. A. Pint and S. Dryepondt
Materials Science and Technology Division, Oak Ridge National Laboratory, Oak Ridge, TN, 37831

Summary
In the 18 month Phase 1 of this project, a facility was assembled for creep testing of refractory metals at 1300°C. This report focuses on the four creep frames that are operational and using an inert gas system (argon) to limit oxidation of the refractory metal specimens being tested. This report details the operations for the first period of operation including the results and lessons learned for Nb- and Mo-based alloy specimens tested by the ORNL team. For an alloy development program, a particularly unique feature of the ORNL facility is more than 40 years of experience conducting mechanical properties testing on sub-sized test specimens (25 mm long dogbones). Due to proprietary constraints, only one representative set of team data are provided. The primary concern for testing Nb-based alloys is oxygen ingress. Despite several strategies to reliably limit O ingress, including getters and Ar gas purity, the experimentally informed strategy currently being developed is a new load train design intended to better seal the system. Hardware for the new design is currently being fabricated.

Introduction

The ORNL facility to support the ARPA-E ULTIMATE program is focused on conducting 100 h creep tests at 1300°C in a reliable and reproducible manner. For the original proposal, the available creep frames were for ambient air creep testing at 1300°C. All of the ULTIMATE teams requesting 1300°C testing wanted the testing done in an inert environment or vacuum. The development of the vacuum creep frame is covered in a second report [1]. This report includes a literature review of Nb alloy mechanical properties, an outline of the approach to achieving creep testing in ultra-high purity (UHP) argon, a summary of results conducted by the ORNL team and lesson learned to date. ORNL testing included Nb alloys CB103 (aka C103, Nb-10Hf-1Ti), Nb-1Zr and Hf carbide strengthened Mo (MHC), which was used to machine the grips. Due to the proprietary nature of the ULTIMATE team research, only one example of team research is included in this report.

Literature Review and Room Temperature Tensile Testing

In preparation for the collection of initial creep data, a literature review was conducted as well as room temperature tensile testing of commercial Nb alloys. Extensive studies have been conducted in the 1950's-1980's to develop and characterize refractory alloys for high temperature applications, with many laboratories involved in long-term creep testing [2-4]. In a technical assessment of Nb-alloys for fusion reactor applications, Pionke and David [2] summarized results from ~250 relevant reports and highlighted three strategies used to improve Nb alloy mechanical properties; solid solution strengthening using W or Mo, dispersion strengthening with elements such as Hf, Zr or Y reacting with interstitial oxygen or carbon to

form oxide or carbide precipitates, and precipitation strengthening with Nb silicide being a key alloy family. As is often the case, alloy strengthening may also result in a decrease in ductility and the ductile to brittle transition temperature (DBTT). For example, the Zr concentration is kept below ~2 wt.% in Nb alloys to avoid a drastic decrease in ductility. Pionke and David also described the impact of key microstructural features such as grain size and precipitate size on the alloy tensile and creep properties. Alloy chemistry plays a key role in controlling these features. Alloy processing, in particular cold/warm working followed by recovery or recrystallization heat treatments, also has a drastic impact on grain and dislocation structures. Recrystallization is often related to significant embrittlement due to segregation of oxygen at grain boundaries during the high temperature heat treatment.

Of the ~46 alloys listed in the report, only a few became actual commercial products with alloy CB-103 being one of the most used Nb-based alloys. The composition (wt.%) of Nb-alloys of interest is summarized in Table 1. Using the 25 mm long dogbone specimens, tensile testing was conducted at room temperature on Nb-1Zr and CB-103 with a strain rate of 0.015/min per ASTM E8-13. The results are compared to literature data in Figure 1. The Nb-1Zr alloy tensile behavior was somewhat more consistent with the other values. The CB-103 specimen exhibited slightly lower strength and higher ductility than expected.

The evolution of the tensile properties of several Nb-based alloys with increasing temperature is shown in Figure 2. Both Nb-1Zr and CB-103 exhibit lower tensile strength but greater ductility in comparison with more advanced Nb-alloys such as F-85, D-43 and C-129Y. At 1300°C, the ultimate tensile strengths of all these alloys are below 200 MPa, the targeted stress for 100 h creep lifetime in the ULTIMATE program. Creep data were gathered for relevant Nb-alloys and Figure 3 shows a Larson Miller plot with data generated at ~1000°-1500°C. The Nb-1Zr and CB-103 alloys exhibited relatively low creep strength at 1300°C, and a stress of ~10-15 MPa would result in a lifetime of ~100 h. (After initial CB-103 testing, the stress level for most experiments was increased to 17.5 MPa. In Figure 3, the best alloys, FS-85 and D-43, exhibited better creep strength but are still far from the targeted performance of the ULTIMATE program. Additional data from Nb-Si-Mo alloys highlight the potential of these alloys with creep strength already exceeding the required target [5].

Table 1: Nb alloys of interest

Alloy	Nominal Composition	Strengthening mechanisms
Nb-1Zr	Nb-1Zr	Dispersion
D-43	Nb-10W-1Zr-0.1C	Dispersion + solid solution
CB103	Nb-10Hf-1Ti-0.7Zr	Dispersion + solid solution
FS-85	Nb-10W-27Ta-0.8Zr	Dispersion + solid solution
Cb-129Y	Nb-10W-10Hf-0.1Y	Dispersion + solid solution
NbSiMo-1	Nb-16Si-5Mo-5W-2.5Hf	Precipitation + solid solution
NbSiMo-2	Nb-16Si-5Mo-15W-5Hf	Precipitation + solid solution

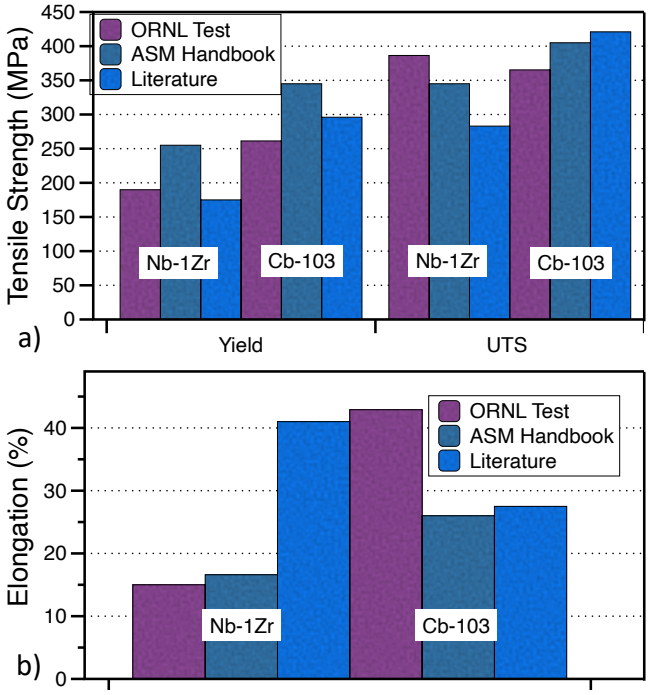

Figure 1, Room temperature tensile properties of Nb-1Zr and Cb-103 alloys, a) Yield and ultimate tensile strength, c) Elongation at rupture.

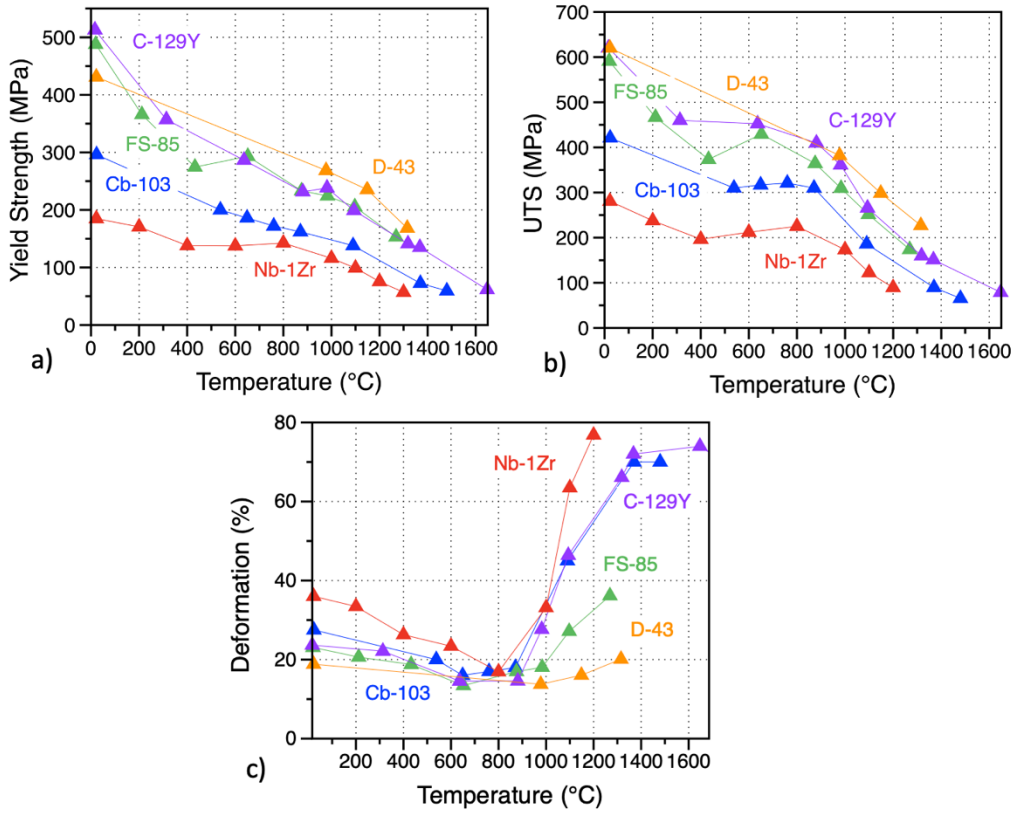

Figure 2: Evolution of the tensile properties of various Nb-based alloys with temperature, a) Yield strength, b) Ultimate tensile strength and c) Elongation at rupture

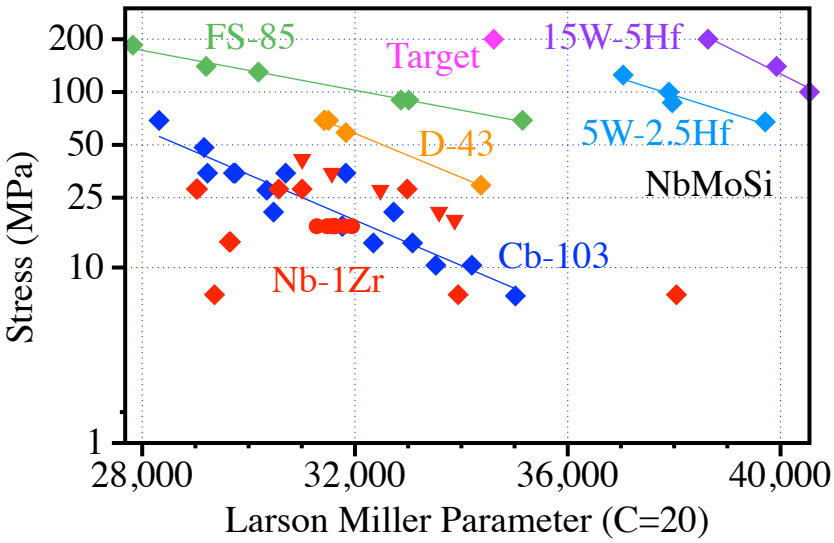

Figure 3: Larson Miller plot for relevant Nb-based alloys at 1000°-1500°C.

Approach to conducting creep testing in an Ar environment

Figures 4-6 show key components of the overhauled mechanical testing platform used to perform creep experiments in Ar at 1300°C. Figure 4a shows one of the starting frames which would normally be configured with an LVDT (linear variable differential transformer) connected to alumina rods contacting the specimen to measure strain during the creep test in ambient air, Figure 4b. With a controlled environment, it is not possible to use an LVDT and displacement of the load train is used to measure strain. The error associated with that is briefly discussed at the end of the report. To comply with DOE and ORNL regulations on electrical equipment and further improve safety during operation, each of the frames was upgraded with controllers certified by a nationally recognized testing laboratory (NRTL). (The frames were not previously NRTL certified.). An example of one of the new controllers is shown in Figure 4c.

Figure 5 shows the major hardware pieces required to build the controlled environment load train system. The primary components are high purity alumina reaction tubes, retorts, pull rods made from Ni-based superalloy MarM247, or 31V and grips. One grip material was high temperature, high strength, oxide dispersion strengthened (ODS) FeCrAl (Plansee alloy PM2000). This is a legacy material available at ORNL. Two more grip materials were Mo alloys, recommended by H. C. Stark, TZM (Mo-0.5Ti-0.1Zr-0.2C) and Mo strengthened by HfC (Mo-1.2Hf-0.1C). Drawings were developed and parts manufactured to enable completion of the 4 overhauled test frames. Because of concern about reaching the 1300°C temperature target, a compact alumina reaction tube and fibrous ceramic gas seals were used at the top and bottom of the load train instead of a long reaction tube and O-rings. The arrow in Figure 5b points to the top fibrous gas seal which is replaced for each creep test. The 25 mm long dog bone specimen has been used at ORNL for many decades and an example is shown in Figure 6a. The

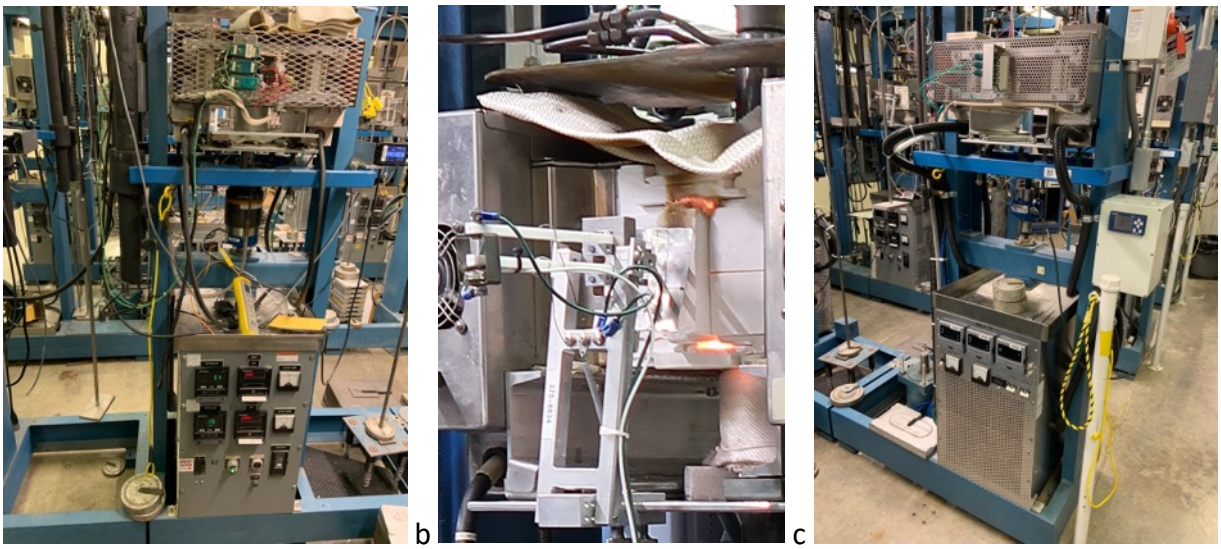

Figure 4. Images of (a) a creep frame before overhaul, (b) LVDT used in ambient air creep frames and (c) a creep frame after overhaul.

specimen's gage section is 2 x 2 mm and drawings were provided to all of the ULTIMATE teams. Because of the reaction tube in the hot section, shorter heating elements were needed, Figure 6b. Procurement of these customized $MoSi_2$ elements delayed the project by more than 3 months. Figure 6c shows a displacement gauge used to measure strain in these experiments.

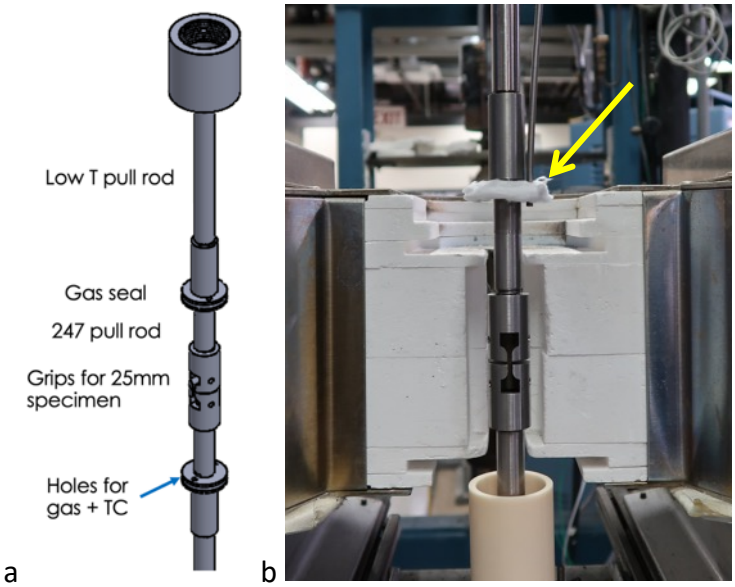

Figure 5. (a) Schematic of the load train and (b) image of the load train which is enclosed in an alumina tube

a 

b 
c 

Figure 6. Images of (a) an example 25mm long dogbone tensile specimen, (b) the shorter $MoSi_2$ heating elements needed for the furnaces when the alumina reaction tube is used and (c) the displacement gauge used to measure strain during these experiments.

It was decided to use the furnace thermocouples to control the temperature, and by the 5th creep test (test 5 in Figure 8), the specimen temperature was steady during the 100 h tests. The tip of the specimen thermocouple was also protected using a ceramic paste to avoid volatilization and limit the thermocouple degradation. Figure 7a shows ODS FeCrAl grips with a loaded specimen and thermocouples attached with Pt wire. The grips are wrapped with either a Ta or Mo foil to further protect the specimen from oxidation, Figure 7b. Initial experiments

a 
b 
c 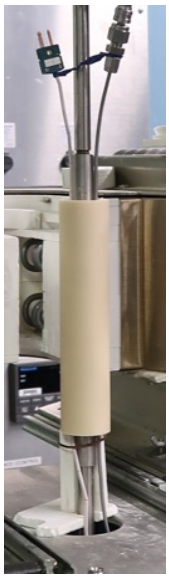

Figure 7. Images of (a) the grips with thermocouples in place, (b) the foil getter and (c) the assembled alumina reaction tube with pull rods.

compared the performance of Mo and Ta foils. The full assembly with the high purity alumina reaction tube in place is shown in Figure 7c.

Figure 8 shows the recorded temperatures during two creep tests of Nb alloy CB103 (Nb-10Hf-1Ti) specimens from the two Pt-Rh Type B thermocouples (TCs) shown in Figure 7a located above (top) and below (bottom) the center of the specimen. Several different strategies were evaluated to control temperature during the initial tests. By the 5th creep test (test 5 in Figure 8), the specimen temperature was relatively steady during the 100 h tests, see Figure 8.

Based on previous ORNL oxidation testing in flowing He with controlled O_2 contents, inlet and outlet oxygen sensors are useful to ensure that an inert atmosphere is being maintained during each creep test and the data from the O_2 sensors can be recorded along with the temperature and displacement data for each experiment. Figure 9 shows the O_2 sensor results from the 5th creep experiment where the gas flow rate was maintained at a sufficient flow rate (0.5 l/min) for the sensor to operate correctly. During the initial experiments, different gas flow rates were used or changed during the test resulting in unexpected changes in the O_2 sensor readings. As expected, O_2 control is extremely important when conducting 1300°C creep experiments on refractory metals and various operating parameters were explored in the next session. The overall performance of the inert gas creep rigs is discussed in the following session on lessons learned.

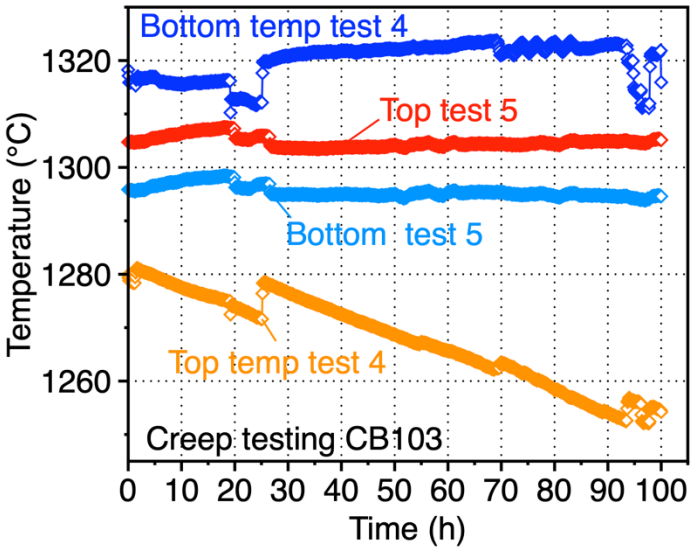

Figure 8. Measure temperature during initial 100 h trial creep tests at #4 and #5. The two specimen thermocouples (top and bottom) are shown in Figure 7a.

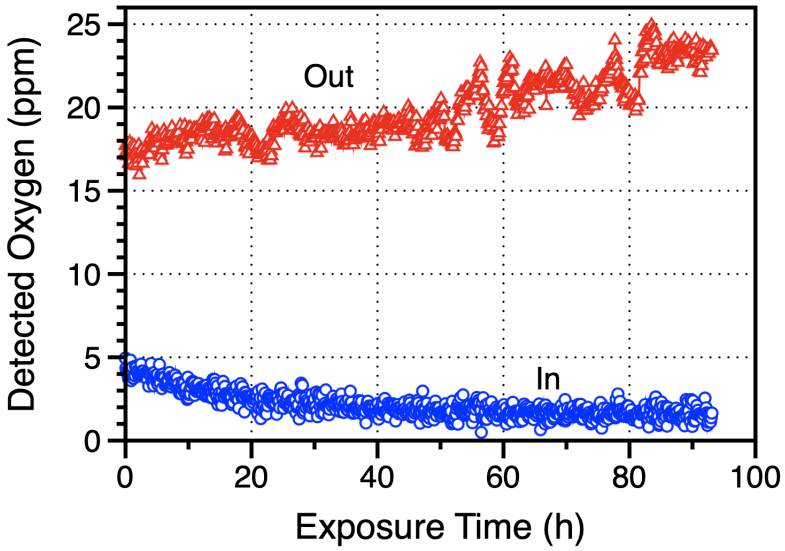

Figure 9. Oxygen content in and out of the reaction tube as a function of exposure time at 1300°C for the 5th creep run.

Inert gas creep testing results

In order to test the operation of the 4 inert gas creep frames in the ORNL facility and complete the calibration and reproducibility milestones, 25 mm long dog bone specimens of CB103, Nb-1Zr and MHC were machined. A summary of the experiments conducted in this phase of testing is shown in Table 2.

After the test procedure was better defined in the first few experiments, including the temperature control procedure, the first metric investigated was Ta versus Mo foil getters to surround the specimen during testing (Figure 7b). Figure 10 shows there was no significant difference observed between Mo and Ta foils but significant variation in creep results. Very high strain rates in two runs in Figure 10a were due to temperature control issues where the extensometer was measuring additional displacement due to temperature variations that were resolved in later experiments. The milestone called for repeating the experiments in triplicate and the strong variations observed are discussed below. Mo and Ta foils were readily available but it was suggested by an ULTIMATE team that Zr would be a better getter. Zr foils were therefore purchase and will be use in the future since Zr is less expensive than Ta or Mo.

From the initial testing, there appeared to be some correlation between the maximum strain measured and the specimen mass gain, which was presumed to be due to O uptake. The Nb alloy specimens became less ductile with increasing mass gain with both Mo and Ta foils, Figure 11. It was initially believed that the range in observations was due to small variations in the gas flow rate or back pressure affecting how O_2 impurities were being controlled. However, repeated testing continued to show variability despite various efforts to reduce O ingress described below.

To confirm the hypothesis about O ingress reducing strain, several Nb alloy creep specimens were metallographically sectioned and the hardness measured along the length of the specimen as an indication of O ingress. The strain/mass gain behavior is shown in Figure 12a

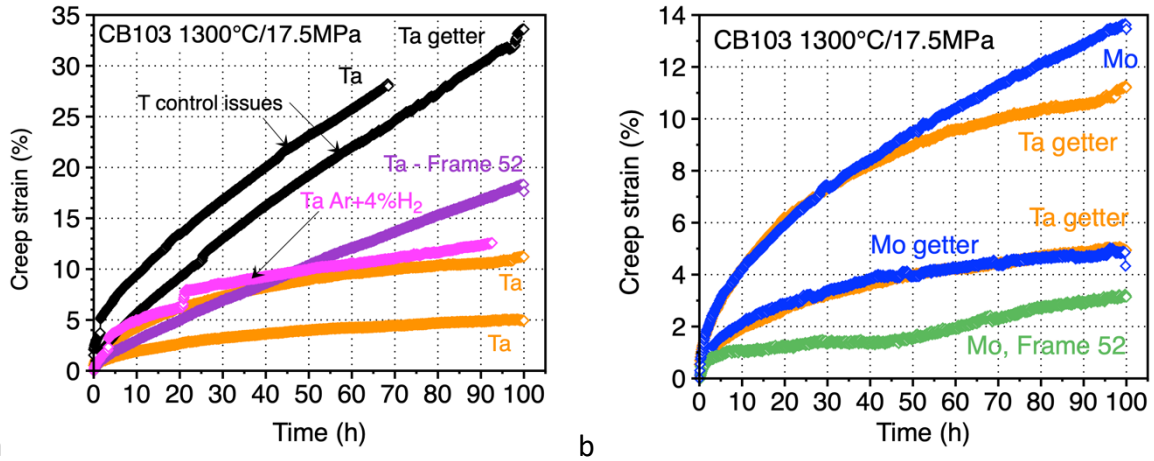

Figure 10. Creep strain for CB103 1300°C tests (a) Ta getter and (b) Mo and Ta getters.

Table 2. Summary of 1300°C creep experiments including the maximum strain measured and the specimen mass gain (SMG) measured after exposure.

Test	Material	Frame	Stress	Gas	Getter	Strain %	SMG mg/cm^2	Notes
1	CB103	75	10,15	UHP Ar	none			Two stress levels
2	CB103	75	17.5	UHP Ar	Ta			Large temp variation
3	CB103	75	17.5	UHP Ar	Mo			Large temp variation
4	CB103	75	17.5	UHP Ar	Ta	33.6	1.87	
5	CB103	75	17.5	UHP Ar	Ta	11.3	7.18	
6	CB103	75	17.5	UHP Ar	Mo	13.6	4.94	
7	CB103	75	17.5	$Ar+H_2$	Ta			Deposits on specimen
8	CB103	75	17.5	UHP Ar	Mo	4.9	8.31	
9	CB103	52	17.5	UHP Ar	Mo			
10	CB103	75	17.5	UHP Ar	Ta	5	8.48	
11	CB103	52	17.5	UHP Ar	Ta	18.3	0.91	
12	Nb1Zr	75	17.5	UHP Ar	Ta			
13	Nb1Zr	75	17.5	UHP Ar	Ta	4.2	5.15	
14	CB103	75	17.5	RG Ar	Ta	6.9	49.80	
15	CB103	52	17.5	RG Ar	Ta	5.5	9.32	
16	CB103	60	17.5	UHP Ar	Ta	2.5	11.29	(25 total tests)
17	CB103	74	17.5	UHP Ar	Ta	5.7	6.95	
18	CB103	60	17.5	UHP Ar	Ta	5.7	10.80	
19	CB103	74	17.5	UHP Ar	Ta	3.2	9.61	
20	CB103	52	17.5	UHP Ar	Ta	4.9	8.40	O_2 getter
21	CB103	75	17.5	UHP Ar	Ta	8.5		O_2 getter
22	CB103	74	17.5	R+ Ar	Ta	8	40.76	
23	CB103	60	17.5	R+ Ar	Ta	2.7	10.28	
24	CB103	60	17.5	UHP Ar	Ta	14.6	0.82	High Ar flow (1 l/min)
25	CB103	74	17.5	UHP Ar	Ta	4.7	17.77	High Ar flow (1 l/min)
26	CB103	75	17.5	UHP Ar	Ta	5.4	8.91	O_2 getter
27	CB103	52	17.5	UHP Ar	Ta	17		O_2 getter/60h rupture
28	CB103	60	17.5	UHP Ar	Ta	3.5	2.36	
29	CB103	74	17.5	UHP Ar	Ta	3.7	6.55	
30	CB103	60	17.5	UHP Ar	Ta	9.2	0.98	High Ar flow (1 l/min)
31	CB103	52	17.5	UHP Ar	Ta	7.4	6.90	
32	MHC	74	60	UHP Ar	Ta	30.4	-0.13	86h rupture
33	MHC	75	60	UHP Ar	Ta	13.4	2.24	
34	MHC	52	60	UHP Ar	Ta	16.1	-0.15	
35	MHC	60	60	UHP Ar	Ta	9.2	0.49	

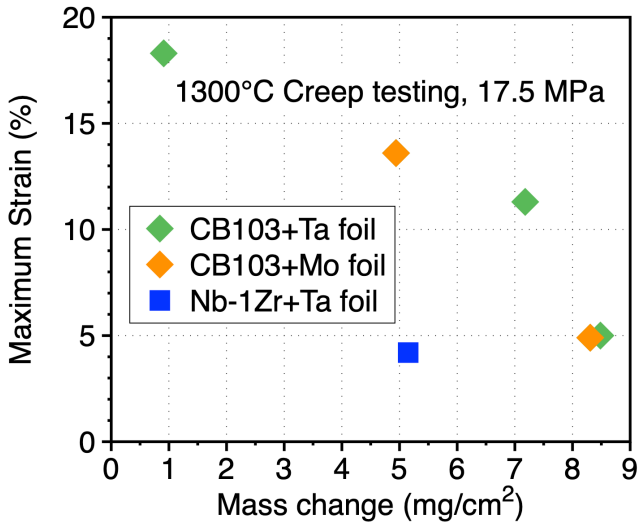

Figure 11. Mass change of Nb alloy specimens plotted versus total strain measured in the 1300°C creep test at 17.5 MPa in flowing argon.

and the hardness profiles are shown in Figure 12b. The lowest hardness values were observed for the as-received specimens of CB103 (blue) and Nb-1Zr (green). After 100 h at 1300°C, some change in hardness may be expected due to thermal ageing. For the specimens with the lowest mass gains, C18 and C20, the change in hardness was minimal. However, higher hardness was observed for the specimens with higher mass gains, especially for the highest mass gain specimen, C17. Thus, there appeared to be some correlation between lower total strain and increased hardness, presumably due to O ingress. However, SEM/EDS (scanning electron microscopy/energy dispersive spectroscopy) maps in Figure 13 showed not only Hf-rich oxide precipitates in CB103 specimen C18 (0.9 mg/cm^2) but evidence of Cr and Fe in the surface layer. This result suggested some interaction between the specimen and the PM2000 (FeCrAl) grips

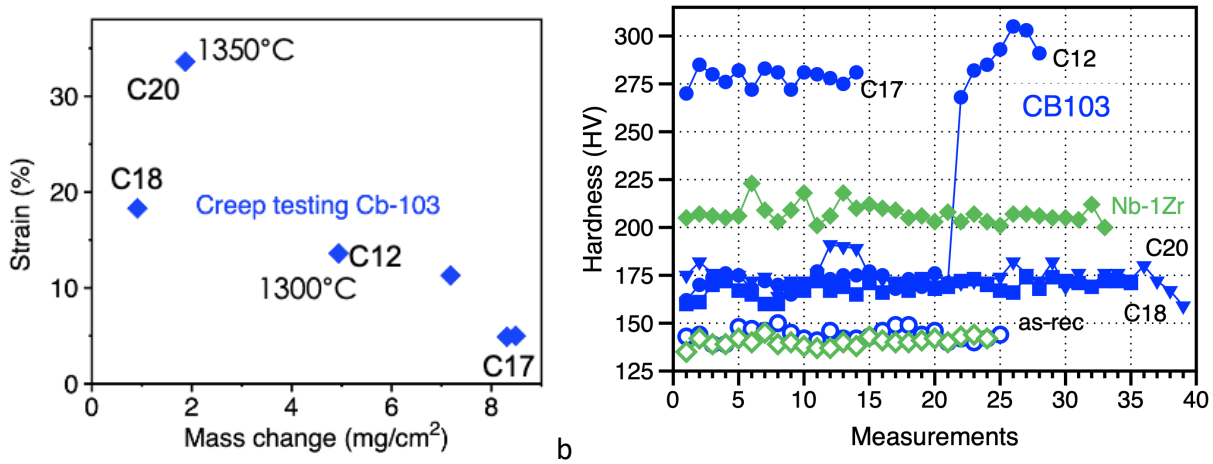

Figure 12. (a) mass change vs. strain for several CB103 specimens (b) hardness along the length of sectioned Nb specimens compared to as-received hardness.

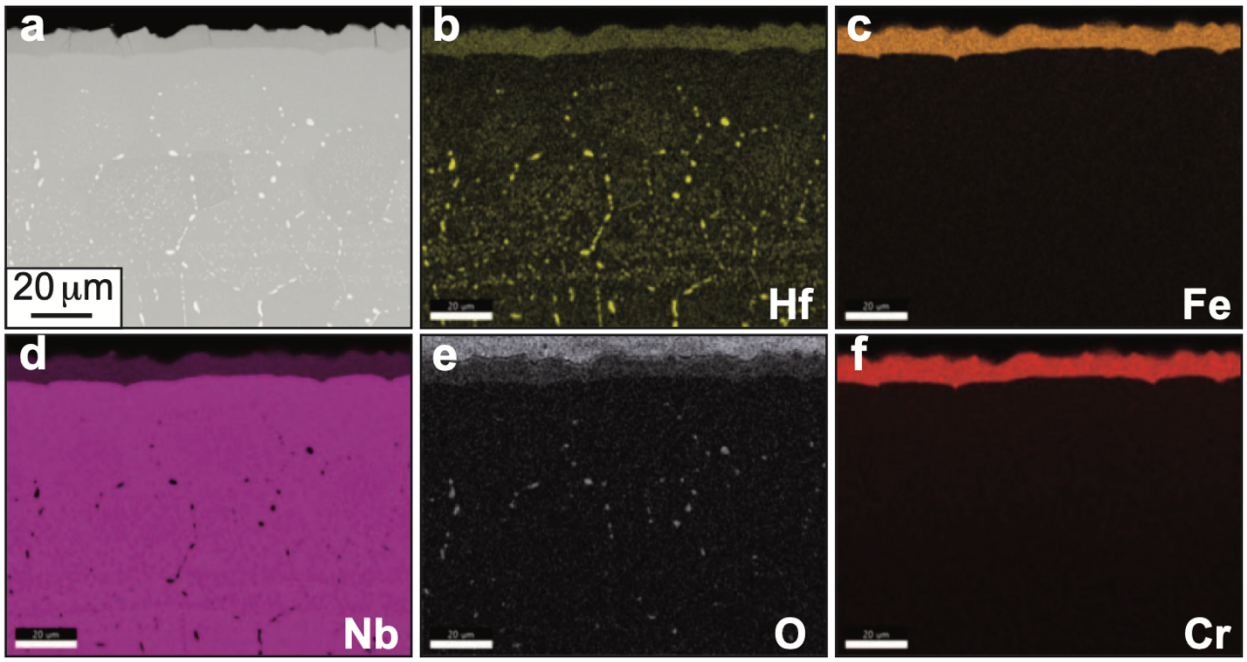

Figure 13. (a) SEM backscattered electron image of polished section of CB103 specimen C18 (0.9 mg/cm^2 mass gain) (b-f) associated EDS maps

that may account for some of the measured mass change. Several specimens were examined and Figure 14 shows a representative example where the Fe- and Cr-rich surface layer was only observed in the grip region in contact with PM2000, Figure 14b, and not in the gage, Figure 14a.

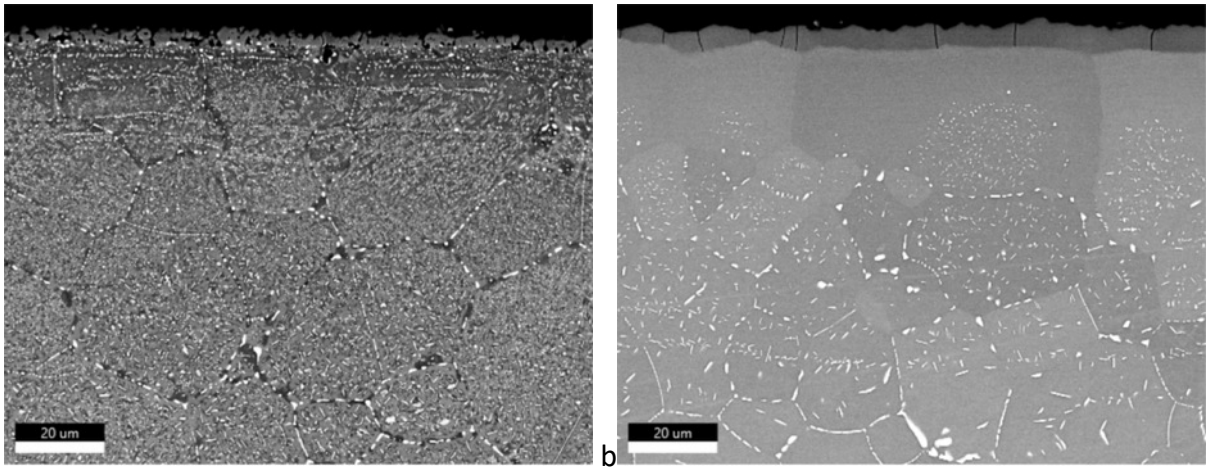

Figure 14. SEM backscattered electron images of specimen C12 showing (a) specimen surface near the fracture in the gage and (b) specimen surface in the grip with a surface layer.

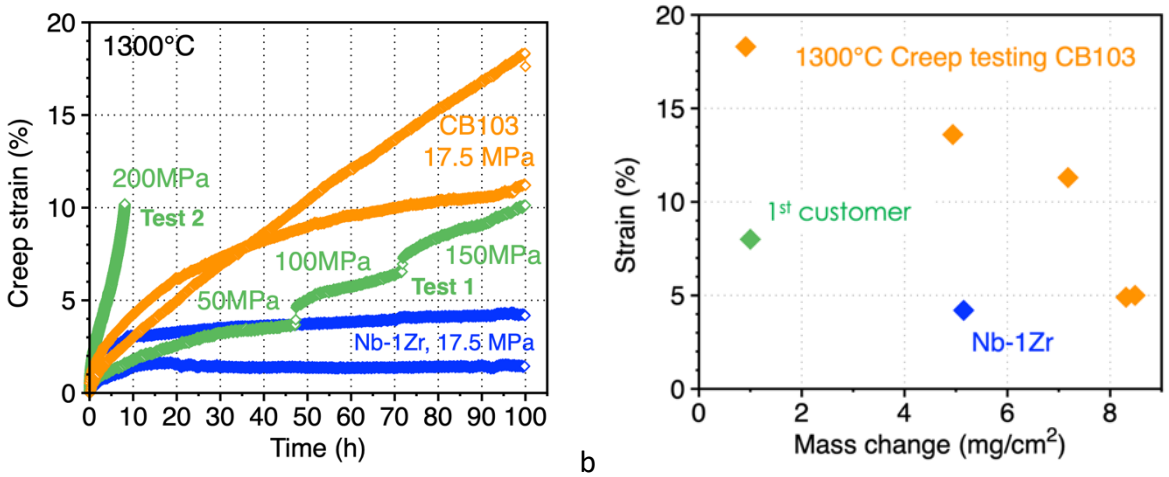

a b

Figure 15. (a) Creep strain for Nb specimens tested at 1300°C with the ULTIMATE team noted in green at a higher stress than the CB103 and Nb-1Zr specimens and (b) mass change for the team specimen was low.

With the procedure better established, initial creep testing for ULTIMATE teams was conducted. Figure 15 shows examples for the first customer where in the first test, the stress was stepped up from 50 MPa to 150 MPa during the 100h test, Figure 15a. The CB103 and Nb-1Zr specimens were tested at a much lower stress but are shown for reference. The mass change for the first customer test was relatively low, Figure 15b. In the second creep test for that customer, the specimen broke under a stress of 200 MPa after less than 10 h. Due to the proprietary nature of the ULTIMATE team research, no additional information team results are included in this report.

Figure 16 summarizes the different gas flow strategies used to reduce specimen mass gain and increase total strain of the CB103 specimens. An initial proposed goal was to compare Ar and Ar-4%H_2 creep results. The Ar-4%H_2 resulted in some evaporation which damaged the specimen and thermocouples and was not repeated. Instead the focus was on different grades of available argon gas shown in Table 3. As shown in Table 2 and Figure 16, the majority of testing was conducted in UHP Ar. Figure 16 also shows that none of the explored changes consistently improved performance by reducing specimen mass gain and increasing total strain. (In some cases, the highest mass gains in Table 2 are not show in Figure 16.) To explore if higher purity argon would be beneficial, Table 3, UHP Ar was replaced by research grade and research plus grade in several experiments, but no clear improvement was observed. Another strategy was to introduce a Ti getter in the gas line to reduce the O_2 level in UHP argon. Figure 16 shows this also did not show a significant benefit. Collectively, these results suggest the fibrous gas seals may be leaking. The final explored option was to increase the gas flow rate from 0.5 to 1 l/min to decrease air leaking into the reaction tube. This showed a benefit in two tests, but not in two others using mass gain and total strain as the performance metrics, Figure 16. In summary, two different getters were used (Ta and Mo) with no difference in performance. Three different argon purity grades were explored and two different gas flow rates. Their effect was not consistently positive.

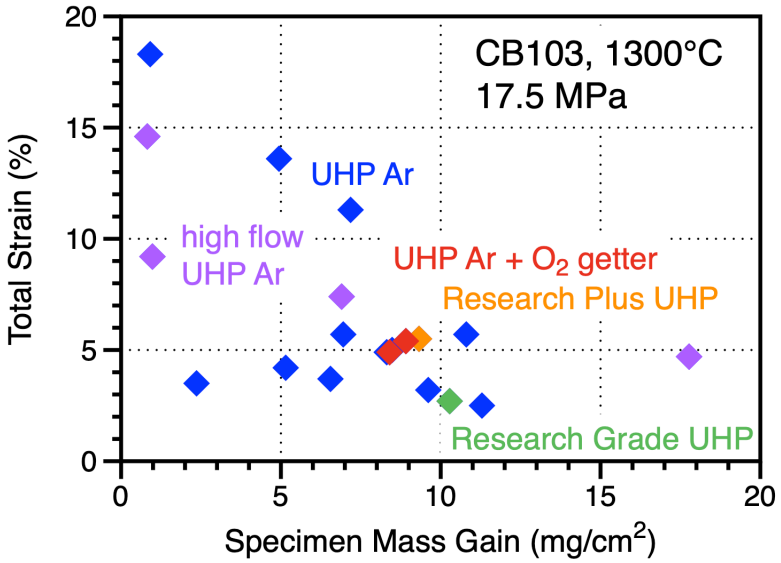

Figure 16. Mass change for Nb-based CB103 specimens versus the total strain measured in the 1300°C creep test at 17.5 MPa.

Finally, Figure 17 shows the results for four 1300°C creep tests at 60 MPa on a HfC-strengthened Mo alloy (MHC). Specimens were run at the same time on the four creep frames (numbered 52, 60, 74 and 75, as noted in Table 2). The tests were conducted using the standard procedure with UHP Ar. Three of the tests were very similar but the fourth specimen ruptured at ~86 h and ~30% elongation. The variability might be attributed to different amounts of O_2 ingress during the experiments.

Table 3. Impurities in grades of Argon used in testing

Gas	O_2 content	H_2O content	Notes
Ultra-high purity (UHP)	<1ppm	<1ppm	Standard gas used in most tests
Research grade (RG)	<0.2ppm	<0.5ppm	>3X increased cost
Research Plus	<0.1ppm	<0.2ppm	>4X increased cost

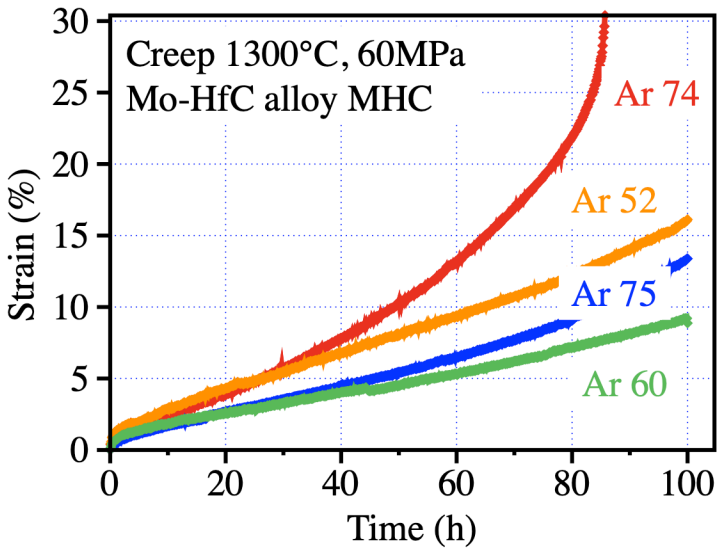

Figure 17. Strain evolution for HfC-strengthened Mo alloys tested in flowing argon at 1300°C and 60 MPa on four different creep frames.

Figure 18 shows images of three of the four specimens. The discoloration is attributed to the ends being in contact with the PM2000 grips. Figure 19 shows SEM backscattered electron images of a polished cross-section through the Mo alloy specimen that ruptured after 86 h. The lower images show the center of the specimen at two different magnifications where the HfC precipitates appear bright because of atomic number contrast. At the surface, the structure the HfC particles appear to be depleted. At higher magnification, smaller precipitates are evident at the surface, which may be HfO_2, but higher resolution characterization is needed.

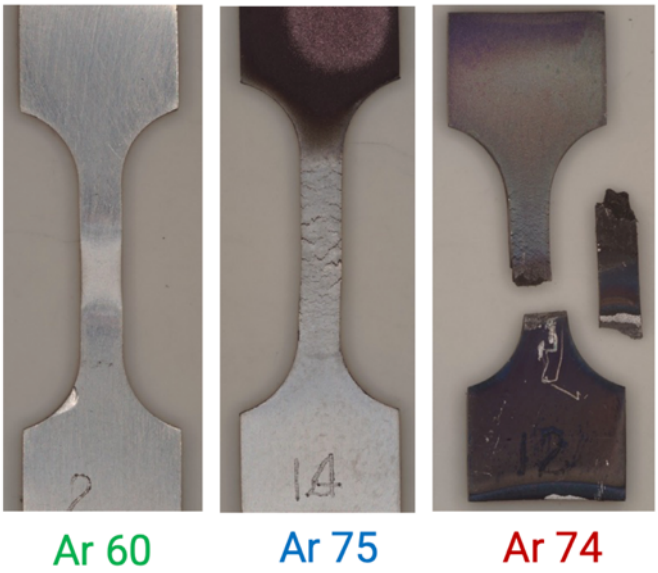

Figure 18. Images of three Mo-HfC specimens creep tested in flowing argon at 1300°C/60 MPa in three different creep frames. Ar-60 had the least deformation.

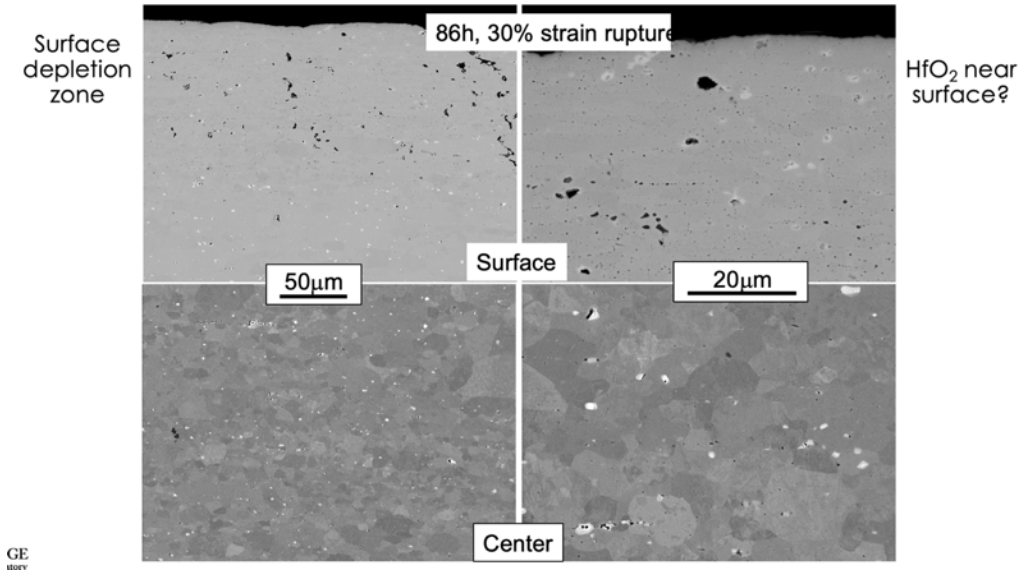

Figure 19. Backscattered electron images of a polished cross-section of the Mo-HfC specimen that ruptured during creep testing at 1300°C/60 MPa. The top images are near the surface at two different magnifications. The lower images are from the center of the specimen.

Lessons Learned

The number one issue identified for 1300°C creep testing in argon during the first phase of operation was O_2 ingress. An initial strategy was the use of a getter to reduce O uptake by Nb-based CB103 specimens. During the initial testing milestones, both Mo and Ta foils were used, Table 2. Figures 10 and 11 show very little difference between Mo and Ta foils. Since the initial experiments, only Ta foil has been used. After the current batch of Ta foil is consumed, Zr foil was purchased and will be used as a potentially less expensive alternative with higher O solubility and better getter performance.

In addition to the foil covering the specimen (Figure 7b), Figure 20a shows an additional Ta foil getter added near where the argon enters the reaction tube. Nevertheless, in some experiments the foil was obviously oxidized after exposure, Figure 20b. Figure 16 summarized the changes in gas purity and flow rate that did not consistently reduce the CB103 specimen mass gain after the 100 h creep test at 1300°C. Table 3 shows that the higher purity Ar grades were significantly more expensive. Increasing the gas flow rate from 0.5 to 1 l/min also required a technician to come into the laboratory on the weekend to change gas bottles. The inconsistent benefit (shown in Figure 16) did not appear to justify the added expense. Because of the inconsistent benefits, combining the more expensive, high purity Ar gas (Table 3) with a higher flow rate was not attempted.

Figure 21 compares the creep curves shown in Figure 17 for Mo-based alloy MHC with the data obtained from a quasi-creep test in vacuum of the same material. The test in vacuum shows a lower creep rate, perhaps due to reduced O ingress.

a b

Figure 20. Images of (a) a second piece of Ta foil getter was added and (b) test where significant getter attacked was observed.

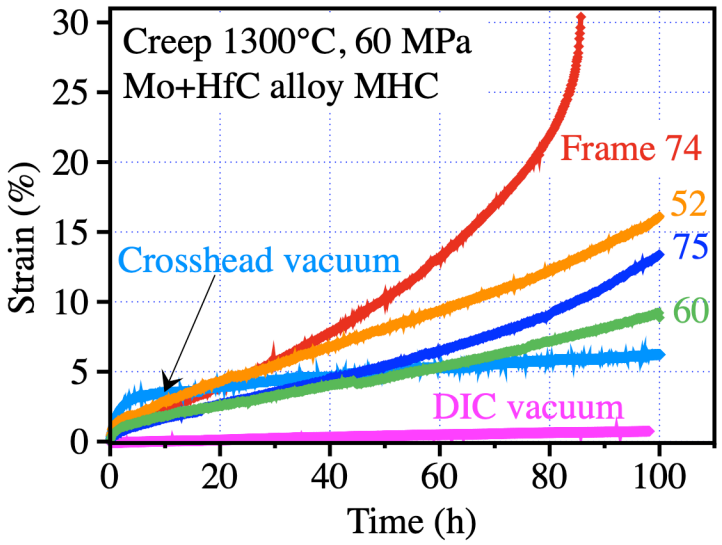

Figure 21. Strain evolution for HfC-strengthened Mo alloys tested in flowing argon at 1300°C and 60 MPa on four different creep frames compared to similar testing in vacuum. The crosshead displacement curve (similar to argon test) is compared to results obtained from digital image correlation (DIC) that optically measured specimen deformation.

To address the O ingress issue, the load train has been redesigned with O-ring seals further from the hot zone, rather than the fibrous seals used in the current design (Figure 5b). Issues are being addressed with purchasing bellows for the new design. Parts for the new design are being machined and are expected to be tested before the end of FY2023. This solution was not initially implemented due to concern on achieving the test temperature of 1300°C. Although the furnaces are rated for temperature up to 1600°C, the presence of an alumina reaction tube decreases the temperature achievable at the specimen surface. With the current configuration, the furnace temperature reached ~1340°C for a specimen temperature of 1300°C. These temperature measurements give us confidence that increasing the length of the reaction tube to allow for O-rings to be used will not impact our ability to perform testing at 1300°C.

In the early stages of testing, temperature control was an issue. The initial experiments focused on maintaining specimen temperature at ~1300°C, which required variation of the furnace control temperature. Figure 22 shows the average temperature results for these experiments comparing the specimen thermocouples (TCs) at the top and bottom of the gage (Figure 7a) and the furnace control TCs for the top and bottom furnaces. For safety, both furnaces also have an over-temperature TC in case the control TC fails. Repeated operation of the first two creep frames during the first two quarters of operation led to concern about TC degradation, especially of the specimen TCs based on the variations shown in Figure 22a. Testing of the specimen TCs after repeated usage did show degradation even though the TCs were protected by a ceramic sheath and the tip was coated with alumina paste. In addition, as the specimen creeps, the location of the thermocouple changes slightly during the experiment.

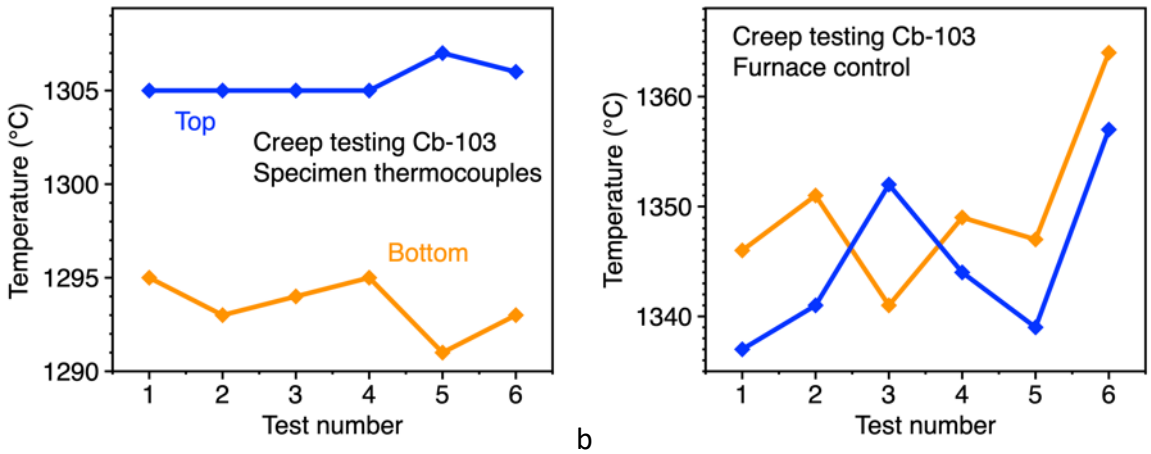

Figure 22. Using the initial control procedure, (a) average specimen temperature in six 1300°C creep tests measured in the top and bottom grips and (b) average control temperature in the same six experiments.

The new temperature control procedure is to determine the furnace control temperature to obtain the specimen at ~1300°C using new specimen TCs that are replaced every 3-4 experiments. Recalibrations of the fully sheathed control and over-temperature TCs showed no degradation with time. The degraded specimen TCs are exposed to flowing gas where evaporation of the TC wire can occur. Evaporation of the control and over-temperature TCs is unlikely in the stagnant environment inside the furnace. Average temperature readings for the new procedure are shown in Figure 23. The control TCs are held constant, Figure 23b. The variability in specimen TCs is attributed to degradation after repeated usage, Figure 23a. Using the control TCs eliminates any safety concerns due to degradation of the specimen TCs and leads to more consistent temperature control.

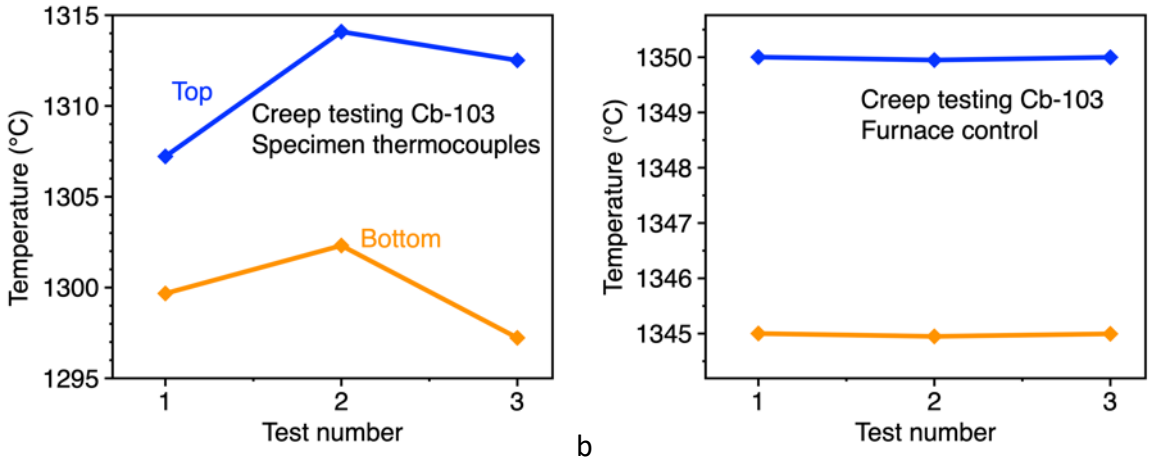

Figure 23. Using the new control procedure (a) Average specimen temperature in three 1300°C creep tests measured in the top and bottom grips and (b) average control temperature in the same three experiments.

a 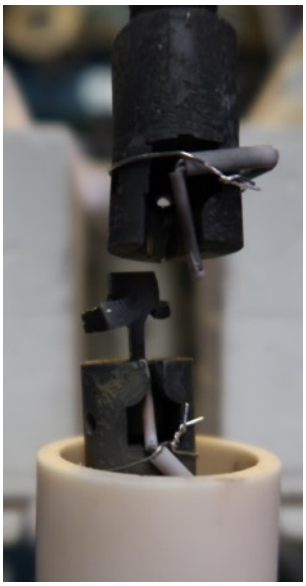 b 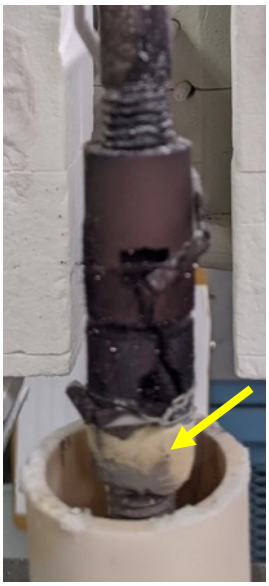

Figure 24. Images of (a) rupture PM2000 grip after 200 MPa testing and (b) damaged MHC grip after a leak occurred. The arrow in (b) shows the heavily oxidized lower grip.

As ULTIMATE team testing began at higher stresses, several lessons were learned. Figure 24a shows a ruptured grip that occurred during testing at 200 MPa. For 200 MPa testing, only Mo-based MHC grips are used. However, MHC can be heavily damaged by oxidation and evaporation if a leak occurs as shown in the lower grip in Figure 24b. The >10 h rupture shown in Figure 15a also led to an unexpected issue. The abrupt motion of the specimen at failure caused the seal to fail and air ingress. The furnace immediately began cooling, but it was ~2 h before the specimen cooled below 100°C. During that period, the getter and specimen were heavily oxidized. To prevent air ingress after rupture, a slightly longer reaction tube was evaluated. That proved successful and that modification was made on all of the frames.

One of the facility goals was to demonstrate sufficient creep frames to conduct 48 creep tests per quarter. With four Ar gas creep frames, this milestone could be completed. For three weeks during one quarter, all four Ar gas frames were operated. During a fourth week, the four MHC creep tests in Figure 21 were conducted. One issue with running multiple frames repeatedly is that there is only 1-2 days between starting and stopping tests each week which can be an issue for scheduling maintenance. While the third and fourth frames were being initially calibrated and tested, it was necessary to stop testing on the first two frames.

Figure 21 also compares the crosshead displacement curve from the vacuum test of MHC to the strain determined by digital image correlation [6,7] (DIC) where specimen deformation is optically measured using a time series of images from a digital camera and a window into the vacuum chamber. As noted earlier, all of the strain measurements in the argon frames use displacement. Thus, there is some error associated with the use of displacement due to compliance of the load train.

Data Handling

To safeguard data generated at the facility, a procedure has been established for addressing intellectual property (IP) issues via a Material Transfer Agreement (MTA) and agreements have been signed with all teams requesting data protection. Also, the teams do not necessarily share the compositions of specimens being tested which limits some IP issues.

References

1. B. A. Pint, M. Ridley and S. Dryepondt, "ULTIMATE FY23 Vacuum Creep Testing Facility Operation Report," ORNL report SPR-2023/1918 (2023) Oak Ridge, TN.

2. L. J. Pionke and David, "Technical Assessment of Niobium Alloys Data Base for Fusion Reactor Applications," DOE Report C00-4247-2 (1979).

3. H.E. McCoy, "Creep properties of selected refractory alloys for potential space nuclear power applications", ORNL report TM-10127 (1986), Oak Ridge, TN.

4. J.A. Horak and L.K. Egner, "Creep properties of Nb-1Zr and Nb-1Zr-0.1C", ORNL report ORNL-6809 (1995).

5. M. Fujikura, A. Kasama, R. Tanaka, and S. Hanada, Effect of Alloy Chemistry on the High Temperature Strengths and Room Temperature Fracture Toughness of Advanced Nb-Based Alloys, Materials Transactions,45, 493 to 501 (2004)

6. K. Kane, S. Bell, B. Garrison, M. Ridley, M. Gussev, K. Linton and N. Capps, "Quantifying deformation during Zry-4 burst testing: a comparison of BISON and a combined *in-situ* digital image correlation and infrared thermography method", Journal of Nuclear Materials, 572, 154063 (2022).

7. K. Kane, B. Garrison, S. Bell, B. Johnston, N. Capps and K. Linton, Report Summarizing Progress in Digital Image Correlation Analysis of Burst Phenomenon, ORNL report TM-2022/2382 (2022).